Yun, X. and Gardner, L. (2017). Stress-strain curves for hot-rolled steels. Journal of Constructional Steel Research. **133**, 36-46.

Stress-strain curves for hot-rolled steels

Xiang Yun[1], Leroy Gardner*[1]

[1]*Department of Civil and Environmental Engineering, Imperial College London, South Kensington Campus, London, UK*

Corresponding author: Prof. Leroy Gardner, Department of Civil and Environmental Engineering, Imperial College London, London, SW7 2AZ, UK. Email: Leroy.gardner@imperial.ac.uk

Abstract

The use of advanced analytical and numerical modelling in structural engineering has increased rapidly in recent years. A key feature of these models is an accurate description of the material stress-strain behaviour. Development of standardised constitutive equations for the full engineering stress-strain response of hot-rolled carbon steels is the subject of the present paper. The proposed models, which offer different options for the representation of the strain hardening region, feature an elastic response up to the yield point, followed by a yield plateau and strain hardening up to the ultimate tensile stress. The Young's modulus E, the yield stress f_y and the ultimate stress f_u are generally readily available to the engineer, but other key parameters, including the strains at the onset of strain hardening and at the ultimate stress, are not, and hence require predictive expressions. These expressions have been developed herein and calibrated against material stress-strain data collected from the literature. Unlike the widely used ECCS model, which has a constant length of yield plateau and constant strain hardening slope, the proposed models, reflecting the collected test data, have a yield plateau length and strain hardening characteristics which vary with the ratio of yield to ultimate stress (i.e. with material grade). The proposed models require three basic input parameters (E, f_y and f_u), are

simple to implement in analytical or numerical models, and are shown herein to be more accurate than the widely employed ECCS model. The proposed models are based on and hence representative of modern hot-rolled steels from around the world.

Keywords: Constitutive modelling, Hot-rolled carbon steels, Material properties, Material modelling, Plasticity, Stress-strain relation, Strain hardening, Yield plateau

1. Introduction

With the increasing use of advanced computational and analytical methods in structural engineering, there is a crucial need for accurate representations of the key input parameters. Development of accurate, yet simple models to describe the full stress-strain response of hot-rolled structural steels is the subject of the present paper. Representation of the full stress-strain curve is particularly important in analytical, numerical or design models for scenarios in which large plastic strains are encountered. Such scenarios include the simulation of section forming [1], the response of structures under extreme loads [2,3], the modelling and design of connections [4,5] and the design of structural elements incorporating inelastic behaviour and strain hardening [6,7].

Although a number of stress-strain models have been developed for hot-rolled carbon steels [8-10], they are either only applicable to a limited strain range or are too complex to be readily implemented in practice. Comprehensive reviews of existing stress-strain models for structural steel have been presented by Huang [9], Foster [11] and Bruneau et al. [12], while a brief overview is presented in the following section. In this paper, two material models for hot-rolled carbon steels are proposed – a quad-linear material model suitable for use in design calculations allowing for yielding and strain hardening and a bilinear plus non-linear hardening model

suitable for incorporation into advanced numerical simulations. The proposed models are based upon and calibrated against data from over 500 experimental stress-strain curves collected from the global literature from 34 individual sources and featuring material produced around the world.

2. Overview of existing stress-strain models and previous work

2.1. General

A typical stress-strain curve of hot-rolled carbon steel subjected to quasi-static tensile load is illustrated in Fig. 1. In the elastic range, the slope is linear and is defined by the modulus of elasticity, or Young's modulus E, taken as 210,000 N/mm^2 for structural steel according to EN-1993-1-1 [13]. The linear path is limited by the yield stress f_y and the corresponding yield strain ε_y, and followed by a region of plastic flow at an approximately constant stress until the strain hardening strain ε_{sh} is reached. At this point, the plastic yield plateau ends and strain hardening initiates. Beyond this point, stress accumulation recommences at a reducing rate up to the ultimate tensile stress f_u and the corresponding ultimate tensile strain ε_u, as illustrated in Fig. 1.

2.2. Existing stress-strain models

Various simplified models have been proposed to represent the material response of hot-rolled carbon steels, among which the linear models can be grouped as (1) elastic, perfectly-plastic, (2) elastic, linear hardening and (3) tri-linear. The elastic, perfectly-plastic model is illustrated in Fig. 2(a), and forms the basis of the current design methods in EN 1993-1-1 [13]. This model is a suitable simplification for scenarios in which strain hardening is not expected to feature (e.g. in the simulation or design of elements whose resistance is dominated by instability) or in which strain hardening is simply ignored. In this model, only two basic material parameters (E and f_y) are needed. The elastic, linear hardening model offers the simplest consideration of

strain hardening, as illustrated in Fig. 2(b), where E_{sh} is the strain hardening modulus. This model considers strain hardening, is included in Annex C of EN 1993-1-5 [14], and has been used throughout the development of the strain-based continuous strength method (CSM), which allows for the beneficial influence of strain hardening on the design of structural metallic elements, including structural carbon steel [6,7,15], aluminium [16,17] and stainless steel [18,19]. However, due to the existence of a yield plateau, this elastic, linear hardening model is less suitable for hot-rolled carbon steels. The next level of complexity of material models after elastic, linear hardening is the tri-linear model which considers both a yield plateau and strain hardening, as shown in Fig. 2(c). Similar to the elastic, linear hardening model, the tri-linear model assumes a constant strain hardening modulus E_{sh} (after the yield plateau), but this does not accurately capture the observed strain hardening behaviour, which shows a progressive loss in stiffness up to the ultimate tensile stress f_u (see Fig. 1).

The Ramberg-Osgood model [20,21] is widely used to describe the rounded stress-strain response of metallic materials such as stainless steels, aluminium and cold-formed carbon steels that have undergone sufficient plastic deformation to eliminate the yield plateau. The Ramberg-Osgood expression is defined by Eq. (1) and features the Young's modulus E, the 0.2% proof stress $\sigma_{0.2}$, which is conventionally considered as an 'equivalent' yield stress, and the strain hardening exponent n. The Ramberg-Osgood model has been shown to be capable of accurately capturing the stress-strain curve up to $\sigma_{0.2}$, but can become inaccurate at higher strains, as demonstrated for stainless steels in [22]. This observation led to several studies aimed at improving the model at large strains [22-24]. Huang [9] proposed a three-stage stress-strain model based on the Ramberg-Osgood expression which includes both a yield plateau (assuming an inclined yield plateau) and strain hardening, as given by Eq. (2), where $\varepsilon_{0.2}$ is the total strain at the 0.2% proof stress, $E_{0.2}$ and E_{st} are the tangent moduli at the 0.2% proof stress

($\varepsilon_{0.2}$, $\sigma_{0.2}$) and the strain hardening point (ε_{sh}, σ_{sh}), respectively, and m_{sh} and m_u are exponents determining the shape of the second and third stages of the curve, respectively. The accuracy of the proposed model was assessed by comparing its predictions with experimental stress-strain curves as well as the predictions from two existing stress-strain models for metals with a yield plateau: Mander's model [25] and a modified power law model [26]. The proposed model could successfully predict the behaviour of hot-rolled carbon steels with a yield plateau over the full strain range up to ε_u. However, it is only suitable for certain steel grades and the predictive equations are considered too lengthy to be implemented in practical design calculations and analytical formulations.

$$\varepsilon = \frac{\sigma}{E} + 0.002\left(\frac{\sigma}{\sigma_{0.2}}\right)^{n} \tag{1}$$

$$\varepsilon = \begin{cases} \dfrac{\sigma}{E} + 0.002\left(\dfrac{\sigma}{\sigma_{0.2}}\right)^{n} & \text{for } \sigma \le \sigma_{0.2} \\ \varepsilon_{0.2} + \dfrac{\sigma-\sigma_{0.2}}{E_{0.2}} + \left[\varepsilon_{sh} - \varepsilon_{0.2} - \dfrac{\left(\sigma_{sh}-\sigma_{0.2}\right)}{E_{0.2}}\right]\left(\dfrac{\sigma-\sigma_{0.2}}{\sigma_{sh}-\sigma_{0.2}}\right)^{m_{sh}} & \text{for } \sigma_{0.2} < \sigma \le \sigma_{sh} \\ \varepsilon_{sh} + \dfrac{\sigma-\sigma_{sh}}{E_{sh}} + \left[\varepsilon_{u} - \varepsilon_{sh} - \dfrac{\left(\sigma_{u}-\sigma_{sh}\right)}{E_{sh}}\right]\left(\dfrac{\sigma-\sigma_{sh}}{\sigma_{u}-\sigma_{sh}}\right)^{m_{u}} & \text{for } \sigma_{sh} < \sigma \le \sigma_{u} \end{cases} \tag{2}$$

2.3. Existing predictions of ε_{sh} and E_{sh}

The strain hardening strain ε_{sh} and the strain hardening modulus E_{sh} are sensitive to a number of factors, including the chemical composition of the material, the cross-section shape, residual stresses caused by the forming process, thermal effects and even the testing machine and control system employed to measure the stress-strain curve. The length of yield plateau has been found to vary with loading direction [27], material grade [28], cross-section shape [29] and location from where the coupon was extracted [30]. With respect to the strain hardening

modulus E_{sh}, variation has been shown to exist with material grade [10,29,31], cross-section shape [29] and the basic definition [32].

A number of studies have been carried out over the past few decades into the determination of values for the two strain hardening parameters ε_{sh} and E_{sh}. Boeraeve et al. [33] proposed a quad-linear material model, using the tangent hardening modulus and recommended values of $E_{sh} = 2\%E$ and $\varepsilon_{sh} = 0.025$ based on the interpretation of a series of experimental stress-strain curves with yield stress ranging from 235 N/mm^2 to 460 N/mm^2. Sadowski et al. [10] presented a statistical analysis of the post-yield material properties of several steel grades and proposed predictive expressions for E_{sh} and the length of yield plateau based on regression analysis. EN 1993-1-5 [14] permits an elastic, linear hardening model with $E_{sh} = 1\%E$ in limit state design using computational methods, and this model has also been employed in the CSM to represent material strain hardening effects [6,7,15-19]. A series of studies have been conducted to develop suitable expressions for defining E_{sh} in the CSM elastic, linear hardening material model on the basis of tensile coupon test data [29] and full cross-section tensile test results [8]. Foster [8] also reported that the yield plateau of full cross-sections in tension was consistently shorter than the corresponding plateau measured in tensile coupon tests, by an average of about 40% and 30% in hot-rolled I-sections and hollow sections, respectively. The ECCS publication [34] recommended a constant strain hardening modulus of $E_{sh} = 2\%E$ together with a strain hardening strain ε_{sh} of $10\varepsilon_y$. This model has been supplemented [35] with a horizontal line at $f = f_u$ and an ultimate strain limit of 15%.

Details of different tri-linear and quad-linear material models can be found in [10,33-35]. The existing predictions of ε_{sh} and E_{sh} show considerable variation, due mainly to the fact that each study has only examined a relatively limited set of steel grades, with data collected from a

narrow range of sources. A thorough assessment of both ε_{sh} and E_{sh}, based on a wider range of existing experimental data sets, is therefore needed and is undertaken herein.

3. Expressions for the proposed standardised stress-strain models

In order to overcome the shortcomings of the existing material models, two new standardised models to represent the yield plateau and strain hardening behaviour of hot-rolled steels are proposed: firstly, a quad-linear stress-strain model, illustrated in Fig. 3, and secondly, a bi-linear plus nonlinear hardening model illustrated in Fig. 4 to capture the gradual loss of stiffness in the strain hardening regime. The quad-linear stress-strain model consists of four stages and can be written over the full range of tensile strains as:

$$f(\varepsilon)=\begin{cases} E\varepsilon & \text{for } \varepsilon \le \varepsilon_y \\ f_y & \text{for } \varepsilon_y < \varepsilon \le \varepsilon_{sh} \\ f_y + E_{sh}(\varepsilon - \varepsilon_{sh}) & \text{for } \varepsilon_{sh} < \varepsilon \le C_1\varepsilon_u \\ f_{C_1\varepsilon_u} + \dfrac{f_u - f_{C_1\varepsilon_u}}{\varepsilon_u - C_1\varepsilon_u}(\varepsilon - C_1\varepsilon_u) & \text{for } C_1\varepsilon_u < \varepsilon \le \varepsilon_u \end{cases} \quad (3)$$

in which $C_1\varepsilon_u$ represents the strain at the intersection point of the third stage of the model and the actual stress-strain curve, and $f_{C_1\varepsilon_u}$ is the corresponding stress, as shown in Fig. 3. The quad-linear model, or the first three stages thereof, is suitable for incorporation into simplified analytical/design approaches that account for strain hardening, and will also provide accurate input for numerical simulations. The bi-linear plus nonlinear hardening model, given by Eq. (4), captures the rounded strain hardening response of hot-rolled steel and will therefore be suitable for advanced numerical simulations of scenarios in which tracing the gradual loss of stiffness is essential. The nonlinear expression adopts a similar form to that proposed by Mander [25], and features four model coefficients (K_1, K_2, K_3 and K_4) which are calibrated

herein based on tensile coupon test data by means of least squares regression. The authors consider the quad-linear model to be appropriate and suitably accurate for the majority of engineering applications.

$$f(\varepsilon)=\begin{cases} E\varepsilon & \text{for } \varepsilon \le \varepsilon_{\mathrm{y}} \\ f_{\mathrm{y}} & \text{for } \varepsilon_{\mathrm{y}} < \varepsilon \le \varepsilon_{\mathrm{sh}} \\ f_{\mathrm{y}} + (f_{\mathrm{u}} - f_{\mathrm{y}}) \left\{ K_1 \left(\dfrac{\varepsilon - \varepsilon_{\mathrm{sh}}}{\varepsilon_{\mathrm{u}} - \varepsilon_{\mathrm{sh}}} \right) + K_2 \left(\dfrac{\varepsilon - \varepsilon_{\mathrm{sh}}}{\varepsilon_{\mathrm{u}} - \varepsilon_{\mathrm{sh}}} \right) \Big/ \left[1 + K_3 \left(\dfrac{\varepsilon - \varepsilon_{\mathrm{sh}}}{\varepsilon_{\mathrm{u}} - \varepsilon_{\mathrm{sh}}} \right)^{K_4} \right]^{1/K_4} \right\} & \text{for } \varepsilon_{\mathrm{sh}} < \varepsilon \le \varepsilon_{\mathrm{u}} \end{cases} \tag{4}$$

In the quad-linear model, two material coefficients, C_1 and C_2, are used. C_1 represents the intersection point discussed previously and effectively defines a 'cut-off' strain to the third stage of the quad-liner model to avoid over-predictions of material strength, while C_2 is used in Eq. (5) to define the strain hardening slope E_{sh}.

$$E_{\mathrm{sh}} = \frac{f_{\mathrm{u}} - f_{\mathrm{y}}}{C_2 \varepsilon_{\mathrm{u}} - \varepsilon_{\mathrm{sh}}} \tag{5}$$

Owing to the progressive loss of stiffness in the strain hardening range (see Fig.1), care must be taken to select a suitable value for the strain hardening modulus E_{sh}. The initial slope method [36], which assumes a constant value of E_{sh} based on the initial post-yield tangent slope taken at $\varepsilon_{\mathrm{sh}}$, is only suitable for the very early stages of the strain hardening region, while assuming linear hardening from $\varepsilon_{\mathrm{sh}}$ to ε_{u} (which corresponds to taking C_2=1), can substantially underestimate the strain hardening over the full tensile strain range. The determination of E_{sh} within the proposed quad-linear material model utilises two defined points on the stress-strain curve: the strain hardening point ($\varepsilon_{\mathrm{sh}}$, f_{y}) and a specified maximum point ($C_2\varepsilon_{\mathrm{u}}$, f_{u}), as shown in Fig. 3. This method has been previously used in the development of the CSM material model

for stainless steel and aluminium, and different values of C_1 and C_2 have been proposed for different materials [19,37,38].

It is desirable to characterize the proposed material models using only the three basic material parameters (E, f_y and f_u), since the values of these parameters are readily available in design codes (e.g. EN 1993-1-1 [13]). Therefore, the other additional material parameters (ε_u, ε_{sh}, C_1 and C_2) need to be expressed in terms of these three basic material parameters. Regression analyses and the development of predictive expressions for the additional material parameters are presented in the subsequent sections of this paper.

4. Experimental database

The experimental database employed herein to underpin the proposed material models comprised over 500 stress-strain curves on hot-rolled steels produced and tested around the world. To establish the predictive expression for ε_u, 347 tensile coupon test results on hot-rolled carbon steels collected from the literature [8,29,35,39-64] and 190 received from the Steel Research Group from the University of Coimbra, from the European project SAFEBRICTILE have been collected and analysed, while a dataset of 455 tensile coupon test results has been collected [8,10,28,29,35,39,40,43-66] to establish the predictive expression for ε_{sh}. A summary of the references for the test data, the number of coupon test results and the steel grades is provided in Table 1. Note that the material parameters f_y, f_u and ε_{sh} determined from [10] were not explicitly reported, and these values were interpreted from the figures of regression lines using digitizing software [67].

The tested coupons were cut either from hot-rolled carbon steel sheets or hot-rolled/finished carbon steel sections, including square hollow sections (SHS), rectangular hollow sections

(RHS), circular hollow sections (CHS), elliptical hollow sections (EHS), angle-sections and I-sections, of various steel grades. These steel grades include S235, S275, S355, S460, S690, S960, Q235, Q345, Q390, Q420 and Q460. Grades S235, S275, S355, S460, S690 and S960 are hot-rolled carbon steels with nominal yield strengths of 235 N/mm^2, 275 N/mm^2, 335 N/mm^2, 460 N/mm^2, 690 N/mm^2 and 960 N/mm^2 respectively, and are specified according to EN 10027-1 [68]. Q235, Q345, Q390, Q420 and Q460 are hot-rolled carbon steels with nominal yield strengths of 235 N/mm^2, 345 N/mm^2, 390 N/mm^2, 420 N/mm^2 and 460 N/mm^2 respectively, and are specified according to GB 50017-2003 [69]. Note that in the Chinese specification GB 50017-2003 [69], Q denotes that the following number in the grade designation is the yield strength.

In the aforementioned references, 235 full-range stress-strain curves were reported and analysed to develop suitable predictive expressions for the material coefficients C_1 and C_2 used in the quad-linear model and to calibrate the four material coefficients (K_1, K_2, K_3 and K_4) employed in the bilinear plus nonlinear hardening model. Development of the predictive expressions for these parameters is described in the following section.

5. Development of predictive expressions for material parameters

The collected data are analysed in this section in order to obtain predictive expressions for the additional material parameters (ε_u, ε_{sh}, C_1, C_2, K_1, K_2, K_3 and K_4) used in the proposed material models, after which the effect of the prediction errors on the accuracy of the models is assessed.

5.1. Predictive expressions for ε_u and ε_{sh}

Rasmussen [22] proposed a predictive expression for the ultimate tensile strain ε_u of stainless steels, as given in Eq. (6), where f_y is taken as the 0.2% proof stress due to the rounded nature

of the stress-strain curve of stainless steel. Arrayago et al. [70] supported the proposals of [22] for austenitic and duplex stainless steel, but proposed a revised predictive model given by Eq. (7) for ferritic stainless steel. Observing a similar trend in the carbon steel data assembled herein, ε_u was also considered to depend on the ratio of yield stress f_y to ultimate tensile stress f_u. The experimental ultimate strains ε_u are plotted against the corresponding f_y/f_u ratios for the data from 537 hot-rolled and 272 cold-formed [41,43,45,71-87] carbon steel tensile coupon tests, as shown in Fig. 5. Note that the cold-formed data covers material extracted from both the flat and corner regions of cold-formed sections.

$$\varepsilon_u = 1 - \frac{f_y}{f_u} \tag{6}$$

$$\varepsilon_u = 0.6\left(1 - \frac{f_y}{f_u}\right) \tag{7}$$

Fig. 5 shows the negative correlation that exists between ε_u and the ratio of f_y/f_u for carbon steels. It may be observed that the hot-rolled and cold-formed data generally follow a similar trend, but once f_y/f_u is greater than a value of about 0.9 for hot-rolled steel (normally for high strength material), ε_u remains almost constant at a value of $\varepsilon_u \approx 0.06$. On the basis of regression analysis, the following predictive expression for ε_u is proposed for hot-rolled carbon steels:

$$\varepsilon_u = 0.6\left(1 - \frac{f_y}{f_u}\right), \quad \text{but } \varepsilon_u \geq 0.06 \text{ for hot-rolled steels} \tag{8}$$

The same expression is proposed for cold-formed material, but without the lower bound of $\varepsilon_u = 0.06$ for $f_y/f_u > 0.9$. Note that the slope of the proposed predictive expression is the same as

that recommended for ferritic stainless steel [70], which may have been anticipated due to the similar basic micro-structure. The predictive expression for ε_u provides good average predictions of the test data, with a mean ratio of the tested to predicted values of ε_u being 1.11, and a moderate coefficient of variation (COV) of 0.27. As indicated in Fig. 5, most (80%) of the hot-rolled carbon steel test data lie within ±40% of the predictions. Note that test data for high strength steels are fairly scarce and more data are required to further verify Eq. (8) for such material.

The test data for the strain hardening strain ε_{sh} are plotted against the ratio of f_y/f_u in Fig. 6, including the full cross-section tension data from Foster et al. [8] and Wang et al. [39]. Based on regression analysis, the following equation is proposed to predict ε_{sh} for hot-rolled carbon steels:

$$\varepsilon_{sh} = 0.1\frac{f_y}{f_u} - 0.055, \quad \text{but } 0.015 \le \varepsilon_{sh} \le 0.03 \tag{9}$$

Using the above equation, the mean value and COV for the ratios of the tested to predicted values of ε_{sh} are 1.06 and 0.29, respectively. As shown in Fig. 6, the coupon test results for ε_{sh} are rather scattered, but the majority (85%) of the test data lie within ±50% of the predictions of Eq. (9). Note that the yield plateau lengths from the full cross-section tensile tests are generally less than those from the coupon tests and thus the predicted yield plateau lengths from Eq. (9) are on the conservative side.

5.2. Predictive expressions and values for model coefficients

A total of 235 measured stress-strain curves, covering a wide range of hot-rolled carbon steel grades, have been collected and analysed to establish expressions for the material coefficients C_1 and C_2 used in the quad-linear model and to calibrate the four material coefficients (K_1, K_2, K_3 and K_4) employed in the bilinear plus nonlinear hardening model. The least squares regression method was used for fitting the third stage of the quad-linear model and the strain hardening range of the nonlinear hardening model to the available experimental stress-strain curves. Since the data points are not, in general, evenly distributed along the measured stress-strain curves, the regression fit will be biased towards the regions of the curve that have the higher concentrations of data. Hence, a curve fitting approach has been employed before using the least squares regression analysis to obtain the material coefficients in order to represent the experimental stress-strain curves with an evenly distributed set of data points.

Since the purpose of the curve fitting was to achieve an accurate description of the strain hardening properties, the data from the elastic and yield plateau regions of the curves (i.e. below ε_{sh}) were discarded for this purpose. The strain hardening region was found to be accurately represented by a 7th order polynomial [10], as given by Eq. (10), where a_1-a_7 forms a set of trial coefficients to be determined. Evenly distributed data points could then be obtained from the fitted polynomial.

$$f(\varepsilon) = f_y + \sum_{k=1}^{7} a_k (\varepsilon - \varepsilon_{sh})^k , \qquad \text{for } \varepsilon_{sh} < \varepsilon \le \varepsilon_u \tag{10}$$

Based on a process of least squares regression to the fitted curves, the following predictive expressions for the material coefficients C_1 and C_2 were obtained:

$$C_1 = \frac{\varepsilon_{sh} + 0.25(\varepsilon_u - \varepsilon_{sh})}{\varepsilon_u} \tag{11}$$

$$C_2 = \frac{\varepsilon_{sh} + 0.4(\varepsilon_u - \varepsilon_{sh})}{\varepsilon_u} \tag{12}$$

Substituting Eq. (12) into Eq. (5), the expression for E_{sh} simplifies to:

$$E_{sh} = \frac{f_u - f_y}{0.4(\varepsilon_u - \varepsilon_{sh})} \tag{13}$$

The strain hardening region of each test curve is plotted in a normalised form in Fig. 7, together with the third and fourth stages of the proposed quad-linear model. As shown in Fig. 7, the predictive expressions for the material coefficients C_1 and C_2 can simply yet accurately reflect the strain hardening behaviour of hot-rolled carbon steel. Good agreement can also be seen between the test curves and the proposed nonlinear model, described by Eq. (4), whose material coefficients (K_1=0.4, K_2=2, K_3=400 and K_4=5) were fitted to the assembled dataset.

5.3. Comparison of experimental values of ε_{sh} and E_{sh} with predictions from proposed and ECCS model

In this section, the collected test results for $\varepsilon_{sh,test}$ and $E_{sh,test}$ have been compared with the predictions of the proposed expressions (Eq. (9) for $\varepsilon_{sh,prop}$ and Eq. (13) for $E_{sh,prop}$) and the values recommended by ECCS [34] ($\varepsilon_{sh,ECCS} = 10\varepsilon_y$ and $E_{sh,ECCS} = 2\%E$). The experimental strain hardening slope $E_{sh,test}$ was determined by minimising the coefficient of variation (COV) between the prediction of a linear function and the measured data within the corresponding region. This effectively defines the hardening region of the stress-strain curve that can be most accurately represented as linear. Key statistical values, including the mean and COV of the

test-to-predicted results, determined from either the ECCS model [34] or the proposal made herein for hot-rolled steels, are summarized in Tables 2 and 3 for ε_{sh} and E_{sh}, respectively. It can be seen from Table 2 that the proposed predictive expression for ε_{sh} (Eq. (9)) provides improved mean predictions of the test data compared to the ECCS model and with reduced scatter (COV). With respect to the strain hardening slope, the ECCS model generally over-estimates E_{sh}, as illustrated Table 3, while the proposed model offers a significantly improved mean prediction of the test data and with lower scatter (COV) when the predicted values of the strain hardening and ultimate strain ($\varepsilon_{sh,pred}$ and $\varepsilon_{u,pred}$) are employed in Eq. (13) for the determination of $E_{sh,prop}$. Similarly accurate mean predictions of E_{sh}, but with further reduced scatter, are obtained when using the measured values of the strain hardening and ultimate strain ($\varepsilon_{u,test}$ and $\varepsilon_{sh,test}$) in Eq. (13), as indicated in Table 3.

5.4. Effect of variations in ε_{sh} and ε_u

The effect of variations in ε_{sh} and ε_u on the predicted stress from the quad-linear stress-strain model at ε = 2% is assessed in this section. A strain of 2% was chosen as representative of the upper level of strains that may be experienced in general structural applications. The quad-linear stress-strain curves have been determined for the combinations of ε_{sh} and ε_u shown in Tables 4 and 5, respectively. In all cases, the basic material parameters were taken as: E = 210000 N/mm^2, f_y = 355 N/mm^2 and f_u = 490 N/mm^2, and the reference values of ε_u = 16.5% and ε_{sh} = 1.7% were determined using Eq. (8) and Eq. (9), respectively. Tables 4 and 5 summarize the percentage variations of the predicted stress at ε = 2% due to the given percentage variations of the predicted values of ε_u and ε_{sh}. According to Tables 4 and 5, a reduction of 40% in ε_u leads to a 1.3% increase in stress at ε = 2%, while a variation of ±50% in ε_{sh} leads to a maximum variation in stress of 5.1% at ε = 2%. These comparisons indicate the accuracy of the proposed model and relative insensitivity to variations in the key predicted

parameters. Comparisons between the proposed models and a series of full range experimental stress-strain curves are presented in the next section.

6. Comparison with experimental stress-strain curves and summary of proposals

6.1. Comparison with experimental stress-strain curves

Sample comparisons between eight representative experimental stress-strain curves and the corresponding predicted curves from the proposed and ECCS material models are shown in Fig. 8. The measured values of only the three basic material parameters (E, f_y and f_u) from the eight coupon tests, as given in Table 6, were used in the predicted material curves. It may be seen from Fig. 8 that consistently good agreement is achieved between the predicted and measured stress-strain curves using the proposed models, whereas the ECCS model [34] shows, in some cases, substantial deviation up to 16% from the observed response. This could be due to the fact that the ECCS model was developed based on lower steel grades produced more than three decades ago and is less suitable for the wide range of modern structural steel grades now in common use. The key advantages of the proposed models over the existing ECCS model are (1) the more accurate predictions of ε_{sh} and E_{sh} and (2) the more accurate representation of the gradual loss of stiffness in the strain hardening region.

6.2. Summary of proposals

The proposed quad-linear and bilinear plus nonlinear hardening material models for hot-rolled carbon steels are summarized as follows:

$$f(\varepsilon)=\begin{cases} E\varepsilon & \text{for } \varepsilon \le \varepsilon_{\mathrm{y}} \\ f_{\mathrm{y}} & \text{for } \varepsilon_{\mathrm{y}} < \varepsilon \le \varepsilon_{\mathrm{sh}} \\ f_{\mathrm{y}} + E_{\mathrm{sh}}(\varepsilon - \varepsilon_{\mathrm{sh}}) & \text{for } \varepsilon_{\mathrm{sh}} < \varepsilon \le C_1\varepsilon_{\mathrm{u}} \\ f_{C_1\varepsilon_{\mathrm{u}}} + \dfrac{f_{\mathrm{u}} - f_{C_1\varepsilon_{\mathrm{u}}}}{\varepsilon_{\mathrm{u}} - C_1\varepsilon_{\mathrm{u}}}(\varepsilon - C_1\varepsilon_{\mathrm{u}}) & \text{for } C_1\varepsilon_{\mathrm{u}} < \varepsilon \le \varepsilon_{\mathrm{u}} \end{cases} \quad \text{(quad-linear model)} \tag{3}$$

$$f(\varepsilon)=\begin{cases} E\varepsilon & \text{for } \varepsilon \le \varepsilon_{\mathrm{y}} \\ f_{\mathrm{y}} & \text{for } \varepsilon_{\mathrm{y}} < \varepsilon \le \varepsilon_{\mathrm{sh}} \\ f_{\mathrm{y}} + (f_{\mathrm{u}} - f_{\mathrm{y}})\left\{0.4\left(\dfrac{\varepsilon - \varepsilon_{\mathrm{sh}}}{\varepsilon_{\mathrm{u}} - \varepsilon_{\mathrm{sh}}}\right) + 2\left(\dfrac{\varepsilon - \varepsilon_{\mathrm{sh}}}{\varepsilon_{\mathrm{u}} - \varepsilon_{\mathrm{sh}}}\right) \Big/ \left[1 + 400\left(\dfrac{\varepsilon - \varepsilon_{\mathrm{sh}}}{\varepsilon_{\mathrm{u}} - \varepsilon_{\mathrm{sh}}}\right)^5\right]^{1/5}\right\} & \text{for } \varepsilon_{\mathrm{sh}} < \varepsilon \le \varepsilon_{\mathrm{u}} \end{cases}$$

(bilinear plus nonlinear hardening model) (14)

$$\varepsilon_{\mathrm{u}} = 0.6\left(1 - \frac{f_{\mathrm{y}}}{f_{\mathrm{u}}}\right), \quad \text{but } \varepsilon_{\mathrm{u}} \ge 0.06 \text{ for hot-rolled steels} \tag{8}$$

$$\varepsilon_{\mathrm{sh}} = 0.1\frac{f_{\mathrm{y}}}{f_{\mathrm{u}}} - 0.055, \quad \text{but } 0.015 \le \varepsilon_{\mathrm{sh}} \le 0.03 \tag{9}$$

$$C_1 = \frac{\varepsilon_{\mathrm{sh}} + 0.25(\varepsilon_{\mathrm{u}} - \varepsilon_{\mathrm{sh}})}{\varepsilon_{\mathrm{u}}} \tag{11}$$

$$E_{\mathrm{sh}} = \frac{f_{\mathrm{u}} - f_{\mathrm{y}}}{0.4(\varepsilon_{\mathrm{u}} - \varepsilon_{\mathrm{sh}})} \tag{13}$$

The values of the key parameters (ε_{u}, $\varepsilon_{\mathrm{sh}}$ and E_{sh}), calculated from the derived predictive expressions, for a series of standard hot-rolled structural steel grades from EN 1993-1-1 [13],

based on nominal material properties and nominal element thickness $t \leq 40$ mm, are given in Table 7.

7. Conclusions

A comprehensive study into the constitutive modelling of hot-rolled carbon steels is presented in this paper. A quad-linear material model and a bilinear plus nonlinear hardening material model, to accurately represent the elastic, yield plateau and strain hardening regimes typically associated with hot-rolled steels have been proposed. The models use the three basic material parameters E, f_y and f_u that are readily available to engineers in material standards, as well as additional material parameters, for which predictive expressions or values have been developed. The predictive expressions for the additional material parameters were calibrated based on a large set of experimental stress-strain data collected from the literature, and are expressed in terms of the basic material parameters. As a result, only the three basic material parameters (E, f_y and f_u) are required to describe full stress-strain curves. The accuracy of the proposed models was assessed by comparing its predictions with available experimental stress-strain curves on hot-rolled carbon steel material. The predicted stress-strain curves are shown to be more accurate than the commonly used ECCS model and in good agreement with experimental stress-strain curves over the full range of tensile strains for both normal strength and high strength hot-rolled carbon steels. The proposed stress-strain curves are suitable for incorporation into analytical, numerical and design models of hot-rolled carbon steel elements.

Acknowledgements

The authors would like to acknowledge the financial support given by the China Scholarship Council (CSC), and to thank Dr. Trayana Tankova from the University of Coimbra for the provision of test data.

REFERENCES

[1] Kuwabara, T. (2007). Advances in experiments on metal sheets and tubes in support of constitutive modelling and forming simulations. International Journal of Plasticity, 23(3), 385-419.

[2] Arablouei, A. and Kodur, V. (2016). Modelling delamination of fire insulation from steel structures subjected to blast loading. Engineering Structures, 116, 56-69.

[3] Chen, A., Louca, L.A. and Elghazouli, A.Y. (2016). Behaviour of cylindrical steel drums under blast loading conditions. International Journal of Impact Engineering, 88, 39-53.

[4] Yang, B. and Tan, K.H. (2012). Numerical analyses of steel beam–column joints subjected to catenary action. Journal of Constructional Steel Research, 70, 1-11.

[5] Sabbagh, A.B., Petkovski, M., Pilakoutas, K. and Mirghaderi, R. (2013). Cyclic behaviour of bolted cold-formed steel moment connections: FE modelling including slip. Journal of Constructional Steel Research, 80, 100-108.

[6] Gardner, L., Wang, F. and Liew, A. (2011). Influence of strain hardening on the behaviour and design of steel structures. International Journal of Structural Stability and Dynamics, 11(5), 855-875.

[7] Liew, A. and Gardner, L. (2015). Ultimate capacity of structural steel cross-sections under compression, bending and combined loading. Structures, 1, 2-11.

[8] Foster, A.S.J., Gardner, L., and Wang, Y. (2015). Practical strain-hardening material properties for use in deformation-based structural steel design. Thin-Walled Structures, 92, 115-129.

[9] Huang, J.F. (2010). Stress-strain models for carbon steels. MSc thesis, Department of Civil and Environmental Engineering, University of Macau, Macau.

[10] Sadowski, A.J., Rotter, J.M., Reinke, T. and Ummenhofer, T. (2015). Statistical analysis of the material properties of selected structural carbon steels. Structural Safety, 53, 26-35.

[11] Foster, A.S.J. (2014). Stability and design of steel beams in the strain-hardening range. PhD thesis, Department of Civil and Environmental Engineering, Imperial College London, UK.

[12] Bruneau, M., Uang, C.M. and Sabelli, S.R. (2011). Ductile design of steel structures. McGraw Hill Professional.

[13] EN 1993-1-1. (2005). Eurocode 3: Design of steel structures - Part 1-1: General rules and rules for buildings. Brussels: European Committee for Standardization (CEN).

[14] EN 1993-1-5. (2006). Eurocode 3: Design of steel structures - Part 1-5: Plated structure elements. Brussels: European Committee for Standardization (CEN).

[15] Gardner, L. (2008). The continuous strength method. Proceedings of the Institution of Civil Engineers-Structures and Buildings, 161 (3), 127-133.

[16] Su, M.N., Young, B. and Gardner, L. (2014). Testing and design of aluminium alloy cross-sections in compression. Journal of Structural Engineering ASCE, 140(9), 04014047.

[17] Su, M.N., Young, B. and Gardner, L. (2016). The continuous strength method for the design of aluminium alloy structural elements. Engineering Structures, 122, 338-48.

[18] Gardner, L., Nethercot, D.A. (2004). Stainless steel structural design: A new approach. The Structural Engineer, 82(21), 21-28.

[19] Afshan, S., Gardner, L. (2013). The continuous strength method for structural stainless steel design. Thin-Walled Structures, 68, 42-49.

[20] Ramberg, W. and Osgood, W.R. (1943). Description of stress–strain curves by three parameters. Technical Note No. 902. National Advisory Committee for Aeronautics, Washington, DC.

[21] Hill, H.N. (1944). Determination of stress-strain relations from offset yield strength values. Technical Note No. 927. National Advisory Committee for Aeronautics, Washington, DC.

[22] Rasmussen, K.J. (2003). Full-range stress–strain curves for stainless steel alloys. Journal of Constructional Steel Research, 59, 47-61.

[23] Quach, W. and Huang, J.F. (2014). Two-stage stress-strain models for light-gauge steels. Advances in Structural Engineering, 17, 937-949.

[24] Mirambell, E. and Real, E. (2000). On the calculation of deflections in structural stainless steel beams: An experimental and numerical investigation. Journal of Constructional Steel Research, 54(1), 109-133.

[25] Mander, J. B. (1983). Seismic design of bridge piers. PhD thesis, University of Canterbury, New Zealand.

[26] Recommendation, R.D. (1990). Tension testing of metallic structural materials for determining stress-strain relations under monotonic and uniaxial tensile loading. Materials and Structures, 23, 35-46.

[27] McDermott, J. F. (1969). Local plastic buckling of A514 steel members. Journal of the Structural Division, 95, 1837-1850.

[28] Kuhlmann, U. (1989). Definition of flange slenderness limits on the basis of rotation capacity values. Journal of Constructional Steel Research, 14, 21-40.

[29] Wang, F.C. (2011). A deformation based approach to structural steel design. PhD thesis, Department of Civil and Environmental Engineering, Imperial College London, UK.

[30] Roderick, J. W. (1951). The behaviour of rolled steel joists in the plastic range. British Welding Research Association.

[31] Byfield, M. P. and Dhanalakshmi, M. (2002). Analysis of strain hardening in steel beams using mill tests. Proceedings of the Third International Conference on Advances in Steel Structure, Hong Kong, China, 139-146.

[32] American Society of Civil Engineers (ASCE). (1972). Plastic design in steel – a guide and commentary, 2nd edition.

[33] Boeraeve, P., Lognard, B., Janss, J., Gerardy, J. and Schleich, J. (1993). Elasto-plastic behaviour of steel frame works. Journal of Constructional Steel Research, 27, 3-21.

[34] Vogel, U. (1985). Some comments on the ECCS publication no. 33: Ultimate Limit State Calculation of Sway Frames with Rigid Joints. Construzioni Metalliche HI, 37, 35-39.

[35] Nseir, J. (2015). Development of a new design method for the cross-section capacity of steel hollow sections. PhD thesis, Université de Liège, Liège, Belgique.

[36] Galambos, T.V. (1998). Guide to stability design criteria for metal structures. John Wiley and Sons.

[37] Buchanan, C., Gardner, L. and Liew, A. (2016). The continuous strength method for the design of circular hollow sections. Journal of Constructional Steel Research, 118, 207-216.

[38] Bock, M., Gardner, L. and Real, E. (2015). Material and local buckling response of ferritic stainless steel sections. Thin-Walled Structures, 89, 131-141.

[39] Wang, J., Afshan, S., Gkantou, M., Theofanous, M., Baniotopoulos, C. and Gardner, L. (2016). Flexural behaviour of hot-finished high strength steel square and rectangular hollow sections. Journal of Constructional Steel Research, 121, 97-109.

[40] Chan, T.M. and Gardner, L. (2008). Bending strength of hot-rolled elliptical hollow sections. Journal of Constructional Steel Research, 64(9), 971-986.

[41] Shi, G., Ban, H. and Bijlaard, F.S. (2012). Tests and numerical study of ultra-high strength steel columns with end restraints. Journal of Constructional Steel Research, 70, 236-247.

[42] Foster, A.S.J. and Gardner, L. (2013). Ultimate behaviour of steel beams with discrete lateral restraints. Thin-Walled Structures, 72, 88-101.

[43] D'Aniello, M., Landolfo, R., Piluso, V. and Rizzano, G. (2012). Ultimate behavior of steel beams under non-uniform bending. Journal of Constructional Steel Research, 78, 144-158.

[44] Liew, A. (2014). Design of structural steel elements with the Continuous Strength Method. PhD thesis, Department of Civil and Environmental Engineering, Imperial College London, UK.

[45] Wilkinson, T. J. (1999). The plastic behaviour of cold-formed rectangular hollow section. PhD thesis, Department of Civil Engineering, University of Sydney, Australia.

[46] Yun, X., Nseir, J., Gardner, L. and Boissonnade, N. (2016). Experimental and numerical investigation into the local imperfection sensitivity of hot-rolled steel I-sections. Proceedings of the 7th International Conference on Coupled Instabilities in Metal Structures, Baltimore, Maryland, November 7-8, 2016.

[47] Shokouhian, M. and Shi, Y. (2015). Flexural strength of hybrid steel I-beams based on slenderness. Engineering Structures, 93, 114-128.

[48] Saloumi, E., Hayeck, M., Nseir, J. and Boissonnade, N. (2015). Experimental characterization of the rotational capacity of hollow structural shapes. Proceedings of the 15th International Symposium on Tubular Structures, May 27-29, 2015, Brazil, 591-594.

[49] Zhao, G.G. (2011). Study on stability of Q345GJ steel axial compressed H-shaped members. MSc thesis, School of Civil Engineering, Chongqing University, Chongqing, China (in Chinese).

[50] Zhou, W.J. (2014). Study on the interactive buckling of welded steel members under axial compression. MSc thesis, Department of Civil Engineering, Tsinghua University, Beijing, China (in Chinese).

[51] Lu, J., Liu, H., Chen, Z. and Liao, X. (2016). Experimental investigation into the post-fire mechanical properties of hot-rolled and cold-formed steels. Journal of Constructional Steel Research, 121, 291-310.

[52] Chen, Y.Y., Wang, H.S., Zhao, X.Z., Hu, J.L., Wang, D.S., Jiang, W.W. and Bao, L.J. (2008). Experimental study on hysteretic behaviour of SRC columns with high ratio of core steel, 29(3), 31-39 (in Chinese).

[53] Qiao, L. (2007). The theoretical and testing research on the buckling behaviours of tapered H-section steel column with thin web. MSc thesis, School of Civil Engineering, Beijing Jiaotong University, Beijing, China (in Chinese).

[54] Qi, H.T. (2014). The static behaviour of steel tube confined concrete columns under axial and eccentric loading. PhD thesis, School of Civil Engineering, Harbin Institute of Technology, Harbin, China (in Chinese).

[55] Yu, H.F. (2010). Aseismic Performance of Welded I Section Steel Bracings and Concentrically Braced Steel Frames. PhD thesis, School of Civil Engineering, Harbin Institute of Technology, Harbin, China (in Chinese).

[56] Cao, W.L. (2014). Study on stability and reliability of Q345GJ steel welded H section flexural members. MSc thesis, School of Civil Engineering, Chongqing University, Chongqing, China (in Chinese).

[57] Yang, X.C. (2013). Local stability study of columns under axial compression at elevated temperatures. MSc thesis, School of Civil Engineering, Chongqing University, Chongqing, China (in Chinese).

[58] Kettler, M. (2008). Elastic-plastic cross-sectional resistance of semi-compact H-and hollow sections. PhD thesis, TU Graz.

[59] Lin, C.C. (2012). Local buckling and design method of high strength steel welded-section members under axial compression. MSc thesis, Department of Civil Engineering, Tsinghua University, Beijing, China (in Chinese).

[60] Ban, H.Y., Shi, G. and Shi, Y.J. (2014). Investigation on design method of overall buckling behaviour for Q420 high strength steel equal-leg angle members under axial compression. Engineering Mechanics, 31(3), 63-71 (in Chinese).

[61] Shi, G., Liu, Z., Ban, H.Y., Zhang, Y., Shi, Y.J. and Wang, Y.Q. (2011). Experimental study on the local buckling of high strength steel equal angles under axial compression. Engineering Mechanics, 28(7), 45-52 (in Chinese).

[62] Bao, C.X. (2012). Research on stable bearing capacity of high strength steel. MSc thesis, School of Civil Engineering, Chongqing University, Chongqing, China (in Chinese).

[63] Ban, H., Shi, G., Shi, Y. and Wang, Y. (2012). Overall buckling behaviour of 460MPa high strength steel columns: Experimental investigation and design method. Journal of Constructional Steel Research, 74, 140-150.

[64] Coelho, A.M.G., Bijlaard, F.S. and Kolstein, H. (2009). Experimental behaviour of high-strength steel web shear panels. Engineering Structures, 31(7), 1543-1555.

[65] Cuk, P. E., Rogers, D. F. and Trahair, N. S. (1986). Inelastic buckling of continuous steel beam-columns. Journal of Constructional Steel Research, 6(1), 21-52.

[66] Luo, S. W. (2013). Study on stability of Q345GJ steel flexural members. MSc thesis, School of Civil Engineering, Chongqing University, Chongqing, China (in Chinese).

[67] GetData Graph Digitizer 2.26. (2013). http://getdata-graph-digitizer.com/.

[68] EN 10027-1. (2005). Designation systems for steels – Part 1: Steel names. Brussels: European Committee for Standardization (CEN).

[69] GB50017-2003. (2003). Code for design of steel structures. Beijing: China Planning Press.

[70] Arrayago, I., Real, E. and Gardner, L. (2015). Description of stress–strain curves for stainless steel alloys. Materials and Design, 87, 540-552.

[71] Gardner, L., Saari, N. and Wang, F. (2010). Comparative experimental study of hot-rolled and cold-formed rectangular hollow sections. Thin-Walled Structures, 48 (7), 495-507.

[72] Yan, J. and Young, B. (2002). Column tests of cold-formed steel channels with complex stiffeners. Journal of Structural Engineering, 128(6), 737-745.

[73] Young, B. and Rasmussen, K.J.R. (1995). Compression tests of fixed-ended and pin-ended cold-formed plain channels. Research Report No. R714, University of Sydney, Australia.

[74] Rasmussen, K.J. (2006). Bifurcation of locally buckled point symmetric columns—Experimental investigations. Thin-walled structures, 44(11), 1175-1184.

[75] Kwon, Y.B. and Hancock, G.J. (1992). Tests of cold-formed channels with local and distortional buckling. Journal of Structural Engineering, 118(7), 1786-1803.

[76] Rogers, C.A. and Hancock, G.J. (1996). Ductility of G550 sheet steels in tension-elongation measurements and perforated tests. Research Report No. R735, University of Sydney, Australia.

[77] Kesti, J. (2000). Local and distortional buckling of perforated steel wall studs. PhD thesis, Helsinki University of Technology, Espoo, Finland.

[78] Kaitila, O. (2004). Web crippling of cold-formed thin-walled steel cassettes. PhD thesis, Helsinki University of Technology, Espoo, Finland.

[79] Gosaye, J., Gardner, L., Wadee, M.A. and Ellen, M.E. (2014). Tensile performance of prestressed steel elements. Engineering Structures, 79, 234-243.

[80] Kim, D.H., Kim, J.H. and Chang, S. (2014). Material performance evaluation and super-tall building applicability of the 800 MPa high-strength steel plates for building structures. International Journal of Steel Structures, 14(4), 889-900.

[81] Rasmussen, K.J.R. and Hancock, G.J. (1995). Tests of high strength steel columns. Journal of Constructional Steel Research, 34(1), 27-52.

[82] Rasmussen, K.J.R. and Hancock, G.J. (1992). Plate slenderness limits for high strength steel sections. Journal of Constructional Steel Research, 23(1), 73-96.

[83] Jiao, H. and Zhao, X.L. (2001). Material ductility of very high strength (VHS) circular steel tubes in tension. Thin-walled structures, 39(11), 887-906.

[84] Tran, A.T., Veljkovic, M., Rebelo, C. and da Silva, L. S. (2015). Resistance of cold-formed high strength steel circular and polygonal sections—Part 1: Experimental investigations. Journal of Constructional Steel Research, 120, 245-257.

[85] Ban, H., Shi, G., Shi, Y. and Bradford, M.A. (2013). Experimental investigation of the overall buckling behaviour of 960MPa high strength steel columns. Journal of Constructional Steel Research, 88, 256-266.

[86] Kyvelou, P., Gardner, L. and Nethercot, D.A. (2015). Composite action between cold-formed steel beams and wood-based floorboards. International Journal of Structural Stability and Dynamics, 15(08), 1540029.

[87] Afshan, S., Rossi, B. and Gardner, L. (2013). Strength enhancements in cold-formed structural sections - Part I: Material testing. Journal of Constructional Steel Research, 83, 177-188.

[88] EN 1993-1-12. (2006). Eurocode 3: Design of steel structures - Part 1-12: Additional rules for the extension of EN 1993 up to steel grades S700. Brussels: European Committee for Standardization (CEN).

[89] EN 10025-6. (2004). Hot rolled products of structural steels - Part 6: Technical delivery conditions for flat products of high yield strength structural steels in the quenched and tempered condition.

Figures:

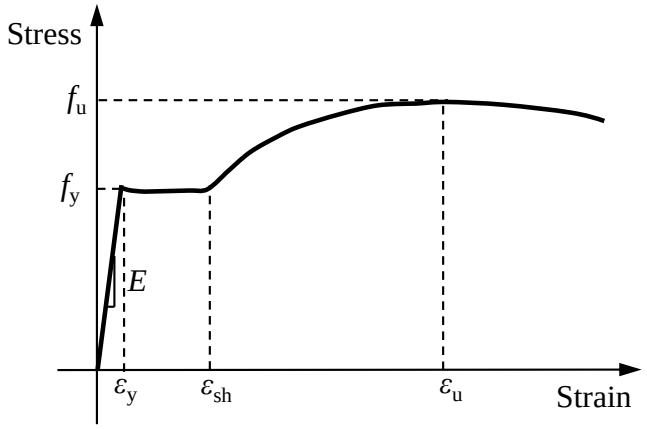

Fig. 1. Typical engineering stress-strain curve for hot-rolled carbon steel.

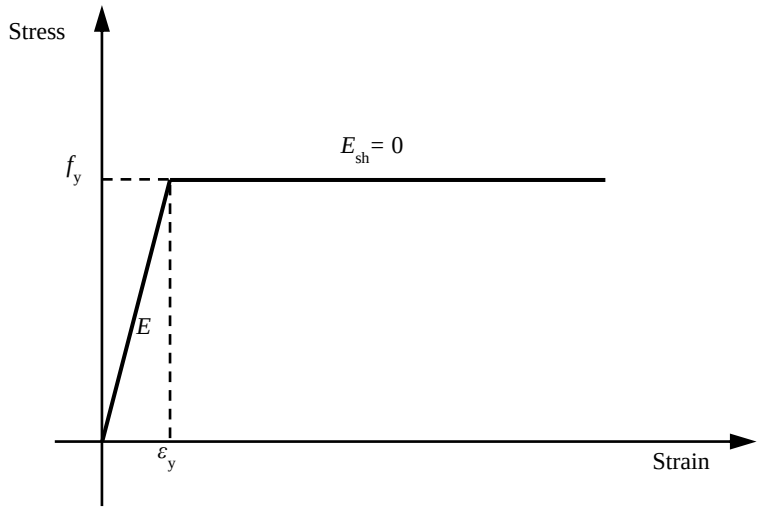

(a) Elastic, perfectly plastic model

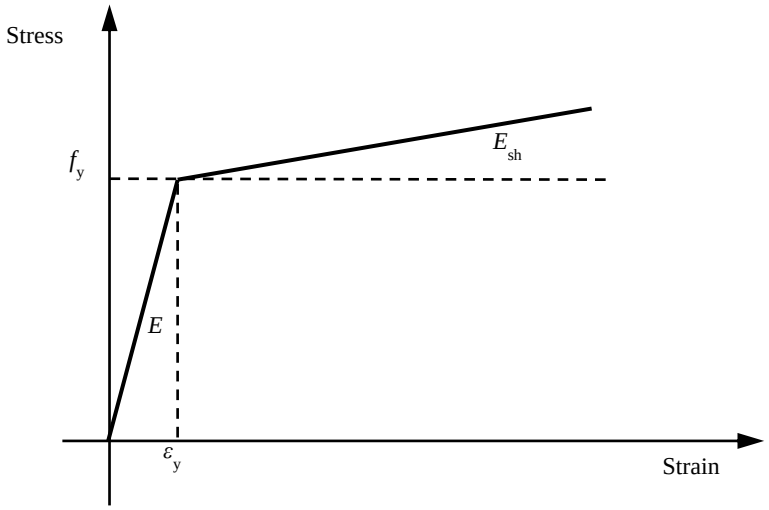

(b) Elastic, linear hardening model

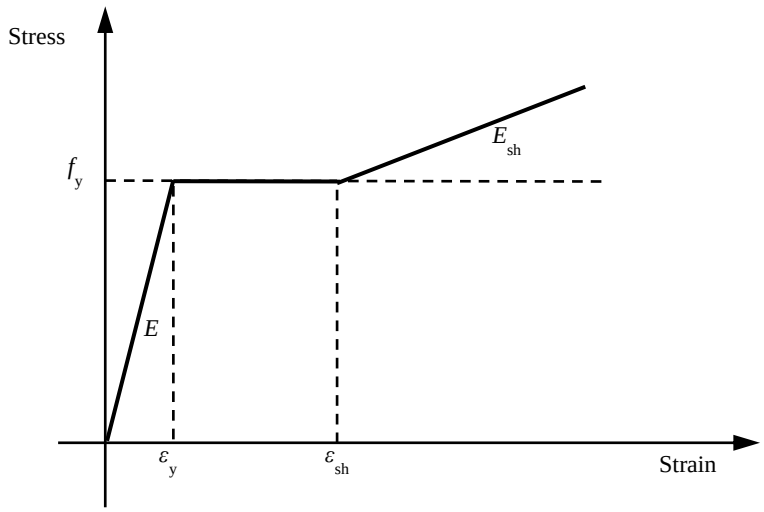

(c) Tri-linear model

Fig. 2. Existing linear material models for hot-rolled carbon steels.

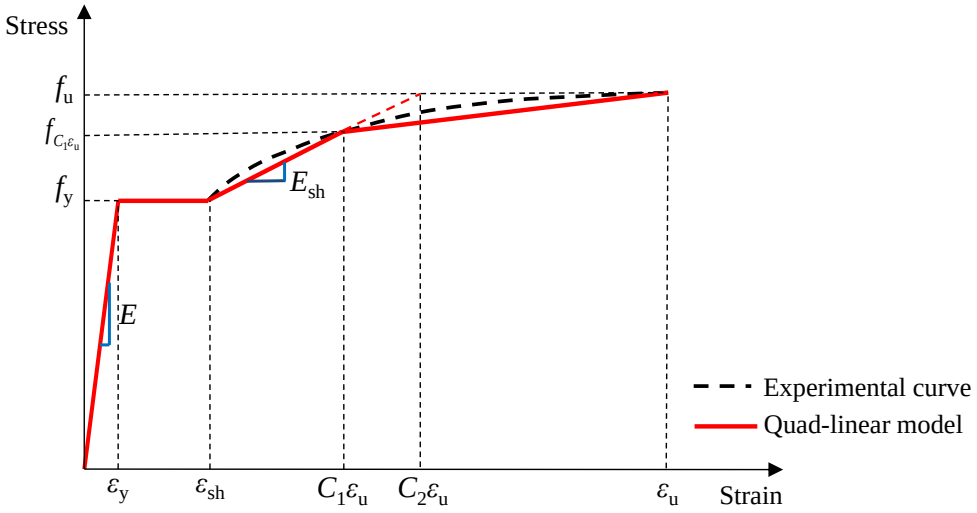

Fig. 3. Proposed quad-linear material model together with typical experimental stress-strain curve.

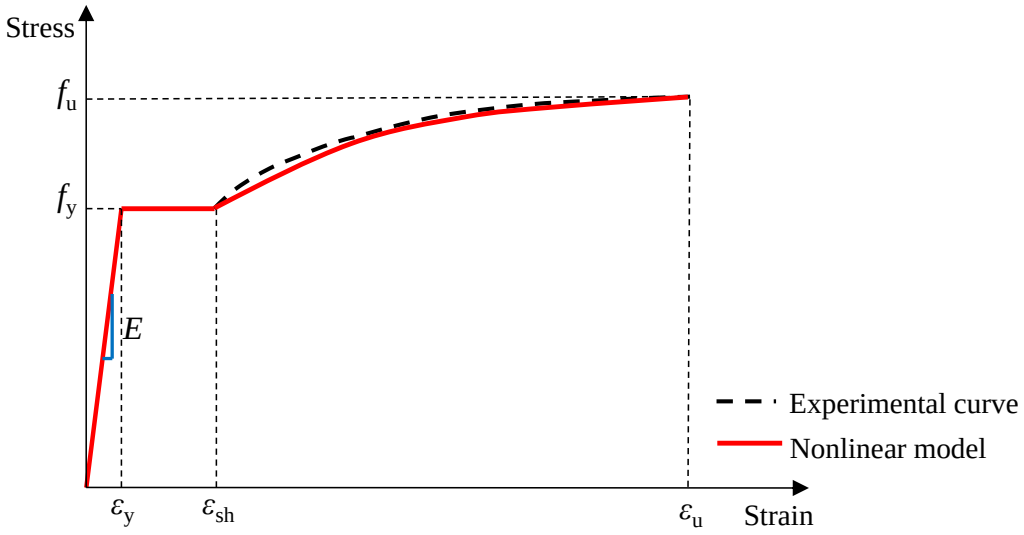

Fig. 4. Proposed bilinear plus nonlinear hardening model together with typical experimental stress-strain curve.

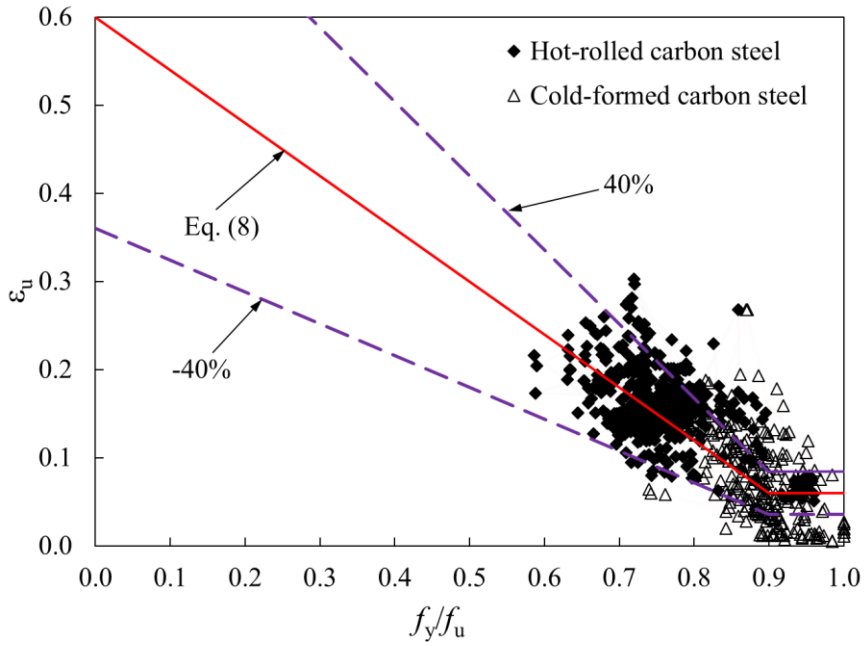

Fig. 5. Evaluation of predictive expression for ε_u for hot-rolled (and cold-formed) carbon steels.

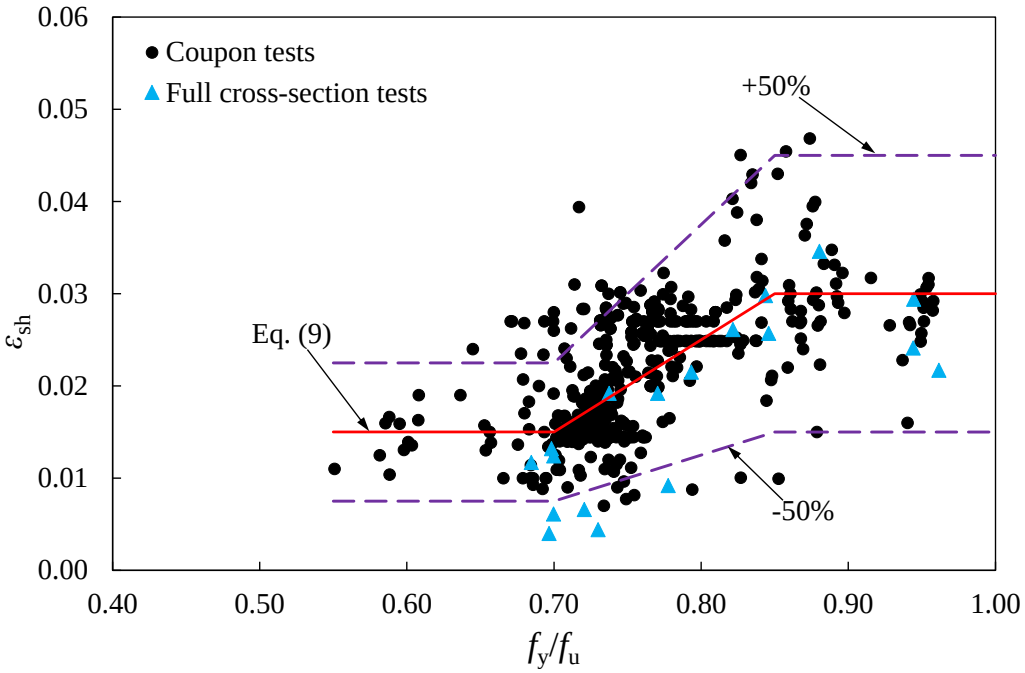

Fig. 6. Evaluation of predictive expression for ε_{sh} for hot-rolled carbon steels.

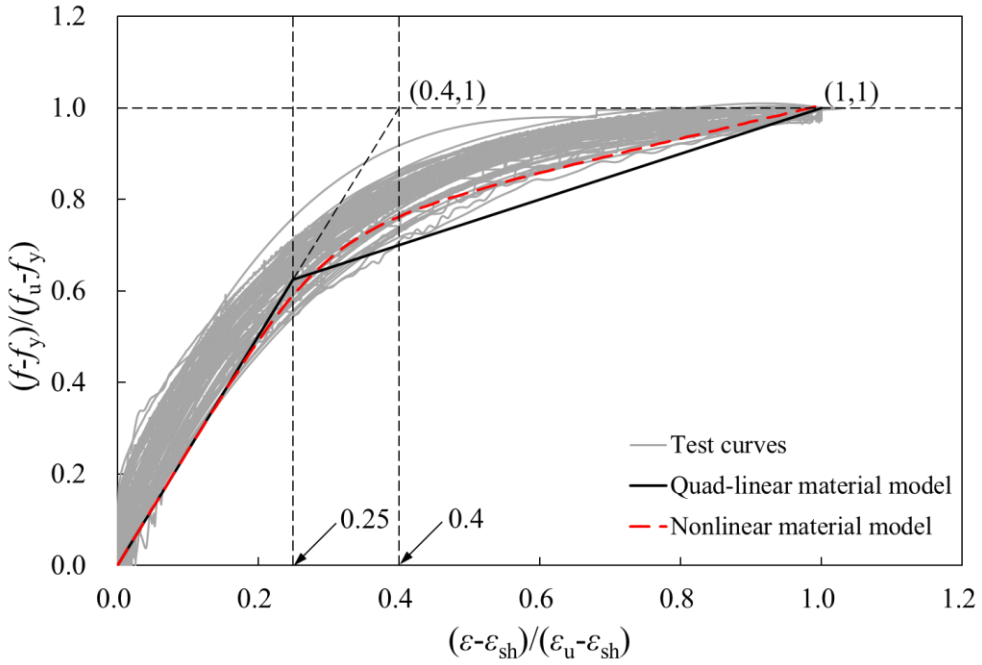

Fig. 7. Comparison between proposed models and experimental stress-strain curves in the strain hardening region.

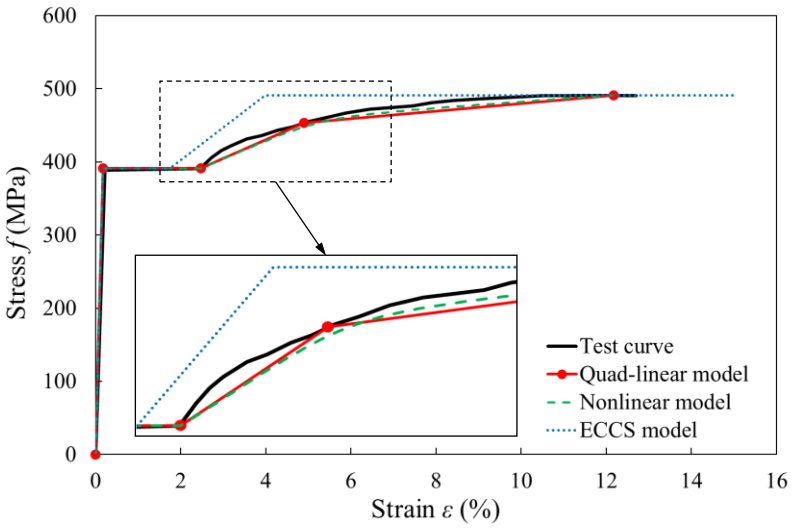

(a) Stress-strain curves predicted by different models for grade S235 specimen cut from I-section tested by Yun et al. [46]

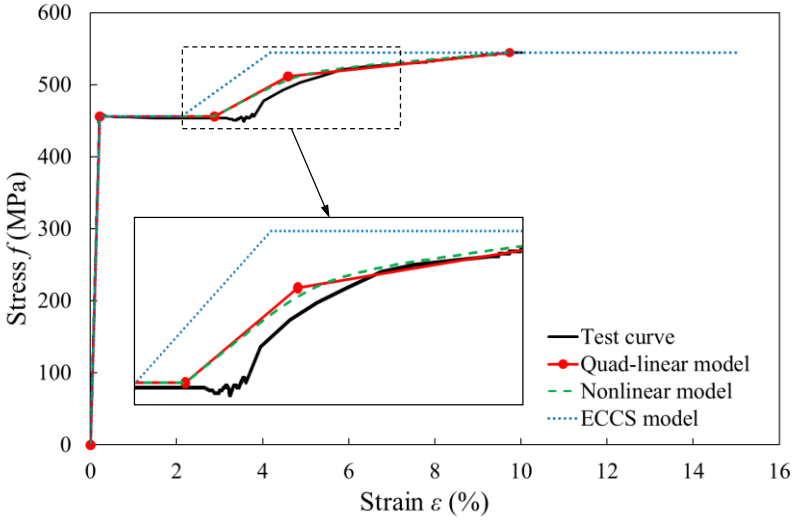

(b) Stress-strain curves predicted by different models for grade S355 specimen cut from SHS tested by Gardner et al. [71]

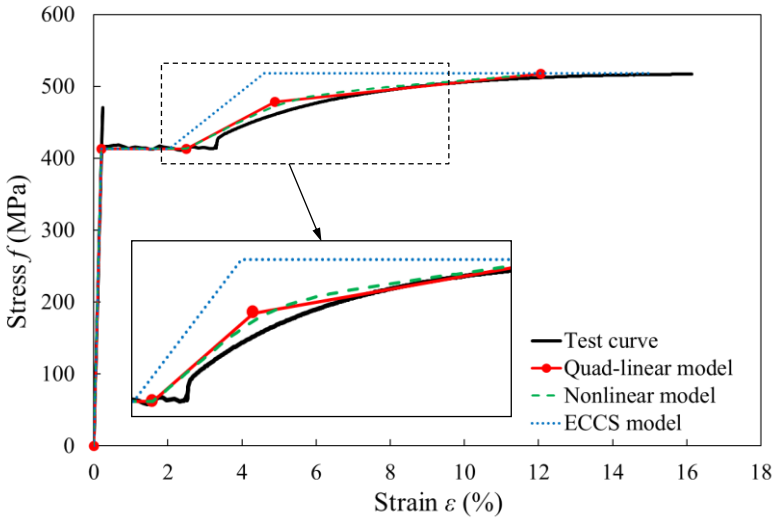

(c) Stress-strain curves predicted by different models for grade S355 specimen cut from RHS tested by Liew [44]

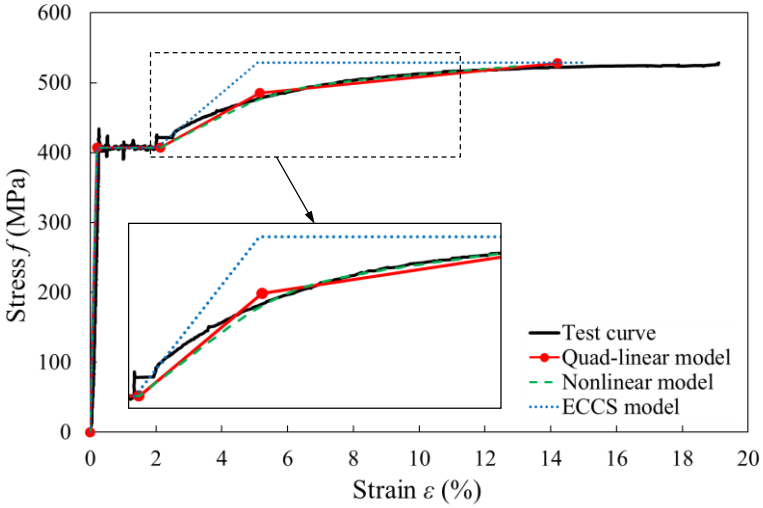

(d) Stress-strain curves predicted by different models for grade S355JR specimen cut from I-section tested by Foster [11]

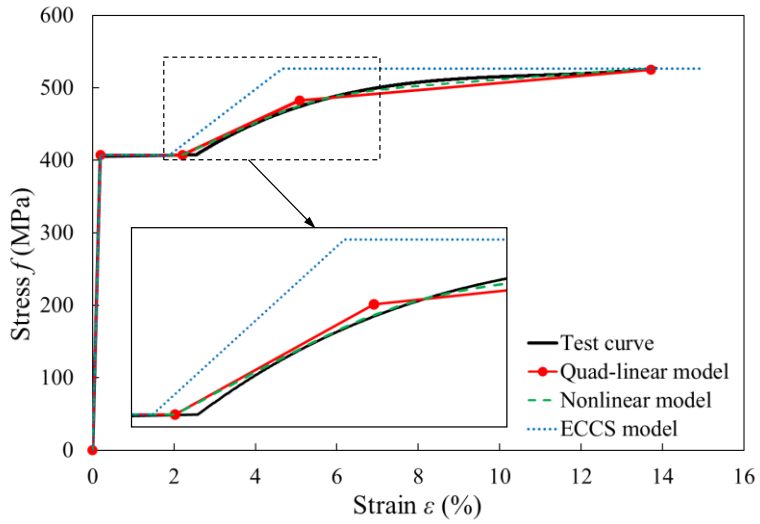

(e) Stress-strain curves predicted by different models for grade S355 specimen cut from EHS tested by Chan and Gardner [40]

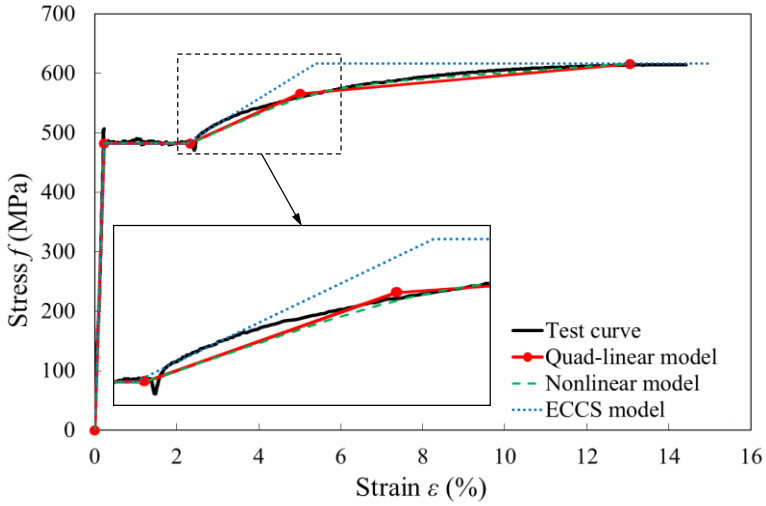

(f) Stress-strain curves predicted by different models for grade S460 specimen cut from SHS tested by Wang et al. [39]

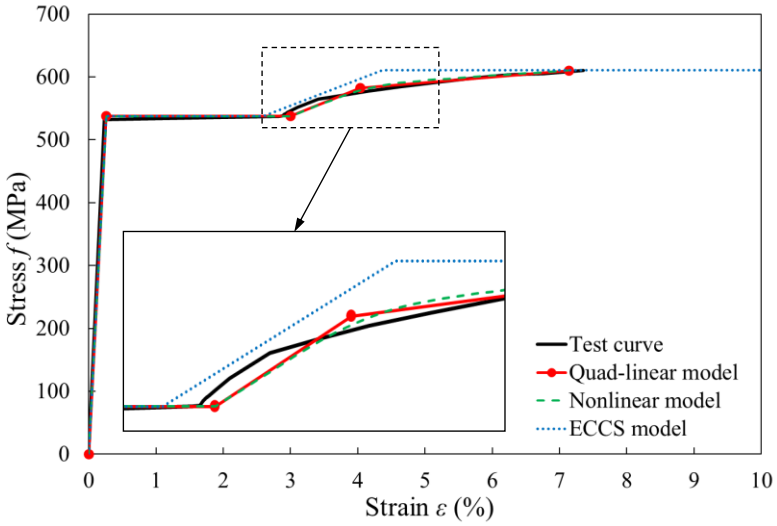

(g) Stress-strain curves predicted by different models for grade S460 specimen cut from steel sheet tested by Shokouhian and Shi [47]

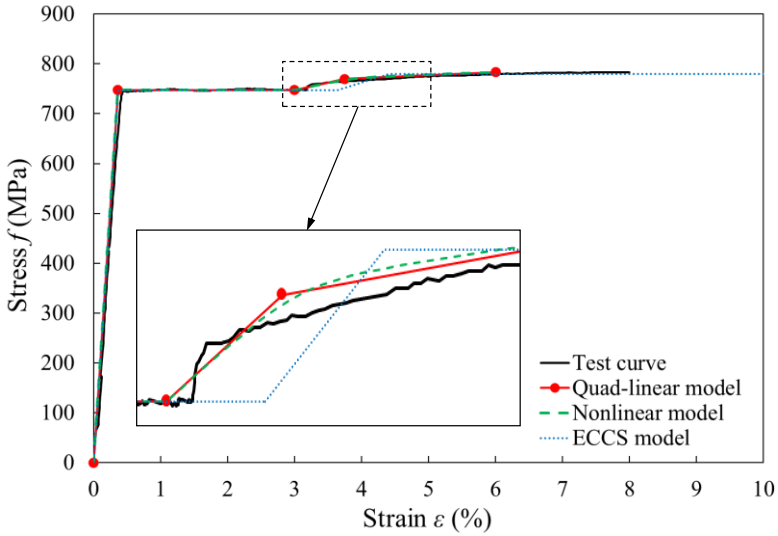

(h) Stress-strain curves predicted by different models for grade S690 specimen cut from SHS tested by Wang et al. [39]

Fig. 8. Comparison of experimental stress-strain curves with the proposed material models and ECCS model.

Tables:

Table 1 Summary of number and details of hot-rolled carbon steel coupon test data used in the development of the proposed material models.

Reference	Steel grade	ε_u	ε_{sh}	Full f-ε curves
[8]	S355[a]	14 (I-sections)	14 (I-sections)	14 (I-sections)
[10]	S235[a]	-	74 (SHS/RHS/CHS/ /sheets)	-
[28]	-	-	10 (sheets)	-
[29]	S355[a]	5 (SHS/RHS)	5 (SHS/RHS)	5 (SHS/RHS)
[35]	S355[a]	6 (RHS)	6 (RHS)	6 (RHS)
[39]	S460[a]/S690[b]	29 (SHS/RHS)	29 (SHS/RHS)	29 (SHS/RHS)
[40]	S355[a]	19 (EHS)	19 (EHS)	19 (EHS)
[41]	S355[a]	7 (I-sections)	-	-
[42]	S355[a]	4 (I-sections)	-	-
[43]	-	9 (I-sections)	9 (I-sections)	-
[44]	S355[a]	31 (RHS)	31 (RHS)	31 (RHS)
[45]	S275[a]	8 (RHS)	8 (RHS)	-
[46]	S235[a]/S355[a]	12 (I-sections)	12 (I-sections)	12 (I-sections)
[47]	Q345[c]/Q460[c]	9 (sheets)	9 (sheets)	9 (sheets)
[48]	S355[a]	61 (SHS/RHS)	62 (SHS/RHS)	61 (SHS/RHS)
[49]	Q345[c]	20 (sheets)	20 (sheets)	-
[50]	Q235[c]/Q345[c]	12 (I-sections/SHS)	12 (I-sections/SHS)	-
[51]	Q235[c]/Q345[c] /Q460[c]	6 (sheets)	6 (sheets)	6 (sheets)
[52]	Q390[c]/Q345[c]	3 (sheets)	3 (sheets)	3 (sheets)
[53]	Q235[c]	8 (sheets)	8 (sheets)	-
[54]	Q235[c]	1 (sheet)	1 (sheet)	-
[55]	Q235[c]	1 (sheet)	1 (sheet)	-
[56]	Q345[c]	24 (sheets)	24 (sheets)	-
[57]	Q235[c]	6 (sheets)	6 (sheets)	-
[58]	S235[a]/S355[a]	22 (I-sections)	22 (I-sections)	22 (I-sections)
[59]	Q460[c]	3 (sheets)	3 (sheets)	3 (sheets)
[60]	Q420[c]	6 (angle-sections)	6 (angle-sections)	-
[61]	Q420[c]	12 (sheets)	12 (sheets)	12 (sheets)
[62]	Q420[c]	2 (sheets)	2 (sheets)	-
[63]	Q460[c]	3 (sheets)	3 (sheets)	3 (sheets)
[64]	S690[b]/S960[d]	4 (sheets)	4 (sheets)	-
[65]	-	-	10 (I-sections)	-
[66]	Q345[c]	-	24 (sheets)	-
Safebrictile Project	S235[a]/S355[a] /S460[a]	190 (I-sections/sheets)	-	-
Total		537	455	235

a: Specified according to EN 1993-1-1 [13]
b: Specified according to EN 1993-1-12 [88]
c: Specified according to GB 50017-2003 [69]
d: Specified according to EN 10025-6: 2004 [89]

Table 2 Statistical results for the ratios $\varepsilon_{sh,test}/\varepsilon_{sh,ECCS}$ and $\varepsilon_{sh,test}/\varepsilon_{sh,prop}$.

	$\varepsilon_{sh,test}/\varepsilon_{sh,ECCS}$	$\varepsilon_{sh,test}/\varepsilon_{sh,prop}$
Mean	1.15	1.06
COV	0.38	0.29

Table 3 Statistical results for the ratios $E_{sh,test}/E_{sh,ECCS}$ and $E_{sh,test}/E_{sh,prop}$.

	$E_{sh,test}/E_{sh,ECCS}$	$E_{sh,test}/E_{sh,prop}$			
		Using $\varepsilon_{u,pred}$ and $\varepsilon_{sh,pred}$	Using $\varepsilon_{u,pred}$ and $\varepsilon_{sh,test}$	Using $\varepsilon_{u,test}$ and $\varepsilon_{sh,pred}$	Using $\varepsilon_{u,test}$ and $\varepsilon_{sh,test}$
Mean	0.67	1.04	1.02	1.09	1.07
COV	0.28	0.26	0.26	0.21	0.17

Table 4 Effect of variation in ε_u on the prediction of stress f at ε = 2% using the quad-linear material model.

ε_u (%)	% change in ε_u	ε_{sh} (%)	f at ε = 2% (N/mm^2)	% change in f at ε = 2%
23.1	40	1.7	359.0	-0.5
19.8	20	1.7	359.8	-0.5
16.5	-	1.7	360.8	-
13.2	-20	1.7	362.5	0.5
9.9	-40	1.7	365.5	1.3

Table 5 Effect of variation in ε_{sh} on the prediction of stress f at ε = 2% using quad-linear material model.

ε_{sh} (%)	% change in ε_{sh}	ε_u (%)	f at ε=2% (N/mm^2)	% change in f at ε = 2%
2.6	50	16.5	355.0	-1.6
2.2	25	16.5	355.0	-1.6
1.7	-	16.5	360.8	-
1.3	-25	16.5	370.3	2.6
0.9	-50	16.5	379.3	5.1

Table 6 Basic material parameters of hot-rolled carbon steels used for comparison.

Reference	Steel grade	Label	E (N/mm^2)	f_y (N/mm^2)	f_u (N/mm^2)	Label
[46]	S235	HEB[1] 160 W[2]	222970	391	491	Fig. 8(a)
[71]	S355	SHS 60×60×3 TF[3]	215200	456	545	Fig. 8(b)
[44]	S355	RHS 120×80×4 TF[3]	203700	413	517	Fig. 8(c)
[11]	S355	UB[4] 305×127×48 W[2]	198700	407	528	Fig. 8(d)
[40]	S355	EHS 300×150×8	215100	407	527	Fig. 8(e)
[39]	S460	SHS 100×100×5 TF[3]	211326	482	616	Fig. 8(f)
[47]	S460	Sheet	206800	537	610	Fig. 8(g)
[39]	S690	SHS 50×50×5 TF[3]	205550	747	783	Fig. 8(h)

[1]HEB: European wide flange H beam
[2]W: tension coupon cut from web
[3]TF: tension coupon cut from flat portion
[4]UB: universal beam of I-shaped cross-section

Table 7 Values of the key parameters from the proposed material model for a series of standard structural steel grades [13].

Steel grade	E	f_y	f_u	ε_y	ε_{sh}	ε_u	$\varepsilon_{sh}/\varepsilon_y$	E_{sh}	C_1
	N/mm^2	N/mm^2	N/mm^2	%	%	%		N/mm^2	
S235	210000	235	360	0.11	1.50	20.83	13.4	1616	0.33
S275	210000	275	430	0.13	1.50	21.63	11.5	1925	0.35
S355	210000	355	490	0.17	1.74	16.53	10.3	2283	0.38
S450	210000	440	550	0.21	2.50	12.00	11.9	2895	0.41